Dielectric Study of the Dynamics of Poly(oxyethylene) Chains in Triblock Copolymers: Poly(oxyethylene)-*b*-polystyrene-*b*-poly(oxyethylene)

Susana Moreno and Ramón G. Rubio*

Department Química Física I, Facultad de Química, Universidad Complutense, 28040-Madrid, Spain

Received October 3, 2001

ABSTRACT: Calorimetric, X-ray scattering, and optical microscopy measurements have been used to characterize the morphology of two PEO-*b*-PS-*b*-PEO copolymers. When the molecular weight of the PS block is much larger than the PEO one, the copolymer does not crystallize from the melt, and two well-separated glass transitions are clearly observed. The glass transition temperatures are different from those of the homopolymers; thus, phase segregation is not complete. For the case of blocks of similar molecular weight, the spherulites fill the whole sample, even if the degree of crystallinity is 60%; thus, the amorphous PS and PEO chains are sandwiched between the lamellae. The dynamics of the PEO chains has been studied by dielectric relaxation. In addition to the structural and the subvitreous relaxation modes, the crystalline copolymer shows a strong high-temperature relaxation that may be attributed to the Maxwell−Wagner interfacial process. It was found that the structure of the polymer does not affect the subvitreous process, but the structural relaxation is strongly dependent on whether the PEO chain is in an amorphous or crystalline sample. The temperature dependence of the relaxation times is compared with that reported in the literature for PS/PEO composites.

Introduction

Block copolymers have attracted much attention during the last years due to their tendency to form ordered structures at the nanometer scale below the so-called order−disorder temperature T_{OD}.[1] Block copolymers formed by crystalline and amorphous blocks lead to materials whose properties are not a simple function of the individual homopolymers, for example, the lamellar thickness in the crystal phase is a function of the degrees of polymerization of both blocks.[2,3] The morphology of these materials is strongly dependent on the crystallization conditions. Depending upon the thermal history and the copolymer structure, either a spherulitic morphology dominated by crystallization or a block copolymer morphology confining the crystalline block into nanoscale domains can be formed. The morphology is strongly influenced by the kinetics, and therefore by the relative values of T_{OD}, T_c, and T_g, where T_c is the crystallization temperature, and T_g the glass transition temperature of the amorphous phase.[4−11] In addition to the crystalline and the amorphous phases, a rigid amorphous phase has been described. This phase is formed by amorphous chains tethered to the crystal structure.[12,13] A recent study of PS-*b*-PEO copolymers has revealed that below the T_{OD}, the rigid amorphous phase contains a significant amount of the PEO chains.[12] This phase has been also described in nonpolymer systems.[14]

Besides their morphology, the dynamics of copolymers also presents specific features. Kotaka and Adachi have carried out extensive studies of noncrystalline copolymers made of polystyrene (PS) and polyisoprene (PI) and found that the dynamics of PI blocks (both segmental and normal modes) in PS-*b*-PI and PI-*b*-PS-*b*-PI copolymers is strongly affected by the morphology of the samples.[15] For temperatures below the T_g of PS, the shape of the dielectric relaxation curves point out that interchain cooperativity increases, and that concerted motions of neighboring tethered chains become important. Also Alig et al.[16] and Vogt et al.[17] have found that even above the T_{OD} the spectrum of segmental relaxation times becomes significantly retarded and broadened as compared to the homopolymers counterparts.

In the case of crystalline copolymers, the structural relaxation may be modified by the presence of the rigid amorphous phase, and if the degree of crystallinity is high enough, by spatial confinement effects.[14,18] However, in a study of poly(oxyethylene)−poly(oxybuthylene) (PEO-*b*-PBO) copolymers, Kyritsis et al.[11] have found that for the structural relaxation, copolymers and homopolymers are characterized by the same distribution of relaxation times. Nevertheless, the distribution of relaxation times is broader in copolymers than in homopolymers in the case of the normal mode. Moreno et al.[19] have studied PEO-*b*-PPO-*b*-PEO (PPO stands for poly(propylene oxide)) copolymers above T_g, and both above and below the melting temperature of PEO, T_m. They found that the distribution of relaxation times of the normal and the segmental relaxations depend on the PEO/PPO relative content.

Copolymers formed by PS and PEO are well suited for the study of the dynamics of PEO chains using dielectric spectroscopy. Since PS is not dielectrically active, only the relaxations of the PEO blocks are observed. In spite that the morphology and the crystallization kinetics of some of these copolymers have been reported,[2,8−10,20,21] the relaxation dynamics has been less studied. Smith et al. have studied the dynamics of PS/PEO composites and ternary composites of PS/PS-*b*-PEO/PEO.[22] Below the T_g of PS, they have reported four relaxation processes. According to the authors, one of the processes associated with the chains in the PEO crystallites. There also are two structural relaxations, one associated with the segmental motions of the

* To whom correspondence should be addressed. E-mail: rgrubio@ quim.ucm.es.

10.1021/ma011732u CCC: $22.00
Published on Web 06/07/2002

Table 1. Characteristics of the Copolymers Used, Where *X* Represents the Crystallinity Fraction Obtained from the DSC Results

copolymer	M_n of blocks	%PEO	M_w/M_n	DSC scan	$T_{g,PEO}$/K	$T_{g,PS}$/K	T_m/K	$100X^a$
P1	2700−18400−2700	23	1.07	1st	216	343	322	35
				2nd	217	331		
P2	3100−2800−3100	69	1.04	2nd	232		323	59

[a] The WAXS technique leads to $X = 0.62$ for the P2 sample after crystallization from the melt.

amorphous PEO chains and the other one with the motions of the rigid amorphous phase (PEO chains tethered to the glassy PS or to the crystals). Finally, they found a subvitreous relaxation that they associated with localized motions in the crystalline chain segments. The presence of a rigid amorphous fraction has been also discussed by Karatasos et al.[13] in the study of amorphous PS-*b*-PI copolymers, and by Mijovic et al. in poly(vinylidene fluoride)−poly(methyl methacrylate) blends.[23] However, it is somewhat surprising that in the results of Smith et al. the intensity of the transition attributed to the rigid amorphous phase is higher that that of the structural relaxation of the amorphous PEO chains.[22]

The aim of the present work is to study the relaxation dynamics of two PEO-*b*-PS-*b*-PEO copolymers with similar PEO block lengths and different PS molecular weights. As a consequence, one of the samples will crystallize from the melt, while the other one will not; the different morphologies will lead to noticeable differences in the relaxation dynamics as observed by dielectric relaxation spectroscopy (DRS).

Experimental Section

The copolymers were obtained from Polymer Source. The molecular weight of the PEG and PS blocks are given in Table 1. Gel permeation chromatography using tetrahydrofuran as solvent was used to determine the overall molecular weight and polydispersity index M_w/M_n; the relative content of the comonomers was obtained by NMR.

The calorimetric measurements reported were carried out at a 10 K/min heating (or cooling) rate in a Mettler Star^e DSC system; the temperature scale was calibrated using *n*-octane, indium, and tin.[24] Two samples were measured for each polymer. The morphology of the PEO-*b*-PS-*b*-PEO copolymers is sensitive to the way in which the samples are prepared. The samples provided by the manufacturer had been dissolved in benzene and precipitated with *n*-hexane, and they were crystalline. A first thermogram for the as-received samples was recorded; in one of the samples, it was rather different from subsequent thermograms recorded after cooling the sample from the melt.

The WAXS experiments were carried out in a Philips X'Pert, MPD model, using Cu Kα radiation; the temperature control was done using an Anton Paar HTK10 chamber. The diffractograms were recorded first by heating the as-received samples, and then cooling after keeping the samples at 383 K for 30 min. SAXS data were obtained using a Kratky chamber (Hecus M. Braun, Graz, Austria). However, the anomalously high noise/signal ratio of the data obtained for these samples did not allowed us to carry out any detailed quantitative analysis. The optical micrographs were obtained with a Jenalab microscope coupled to a Mettler FP82HT heating stage.

The dielectric experiments were done using a Solartron 1260 gain-phase analyzer with a Chelsea dielectric interface. The samples (around 0.3 mm thick) were introduced in a homemade parallel-plate capacitor together with three ceramic spacers (0.2 mm thick). The capacitor was kept under vacuum for 2 days at room temperature and, afterward, at 383 K for 1 day more in order to erase the previous thermal history. Then the samples were cooled to the lowest temperature while pressing before the dielectric experiments were started. This process was important in order to ensure that the geometry of the sample was the one dictated by the spacers, especially in the crystalline sample for which contraction takes place when cooling below the T_m.

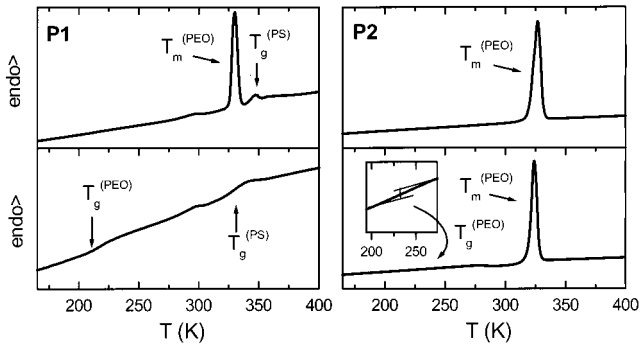

Figure 1. DSC thermograms for the two PEO-*b*-PS-*b*-PEO copolymers studied in this work: left part, P1 sample; right part, P2 sample. The upper part corresponds to the as-received samples, and the lower part corresponds to the samples cooled from the melt. The inset shows the glass transition of the PEO blocks in an enlarged scale.

A home-built cryostat−thermostat was used, which allowed the temperature to be constant within ±0.2 K at 200 K and ±0.1 K above 250 K. The global lineal-frequency window available to our experiments is 10^{-2}−10^6 Hz. All the measurements were carried out in the isothermal mode.

Results

Figure 1 shows the thermograms obtained for the two samples studied in this work; as can be observed, the first heating scan of sample P1, corresponding to the as-received sample, shows two glass transitions corresponding to the PEO and the PS blocks and an intense peak due to the melting of the PEO crystals. The second heating shows two well-separated glass transitions, which confirms the immiscibility of the blocks. The values of the T_g for the PEO-rich phase is similar to those reported for the PEO−PPO−PEO copolymers.[19] Due to the broad interval of T_g's reported for pure PEO,[25,26] it is difficult to draw quantitative conclusions about the miscibility of the blocks from these results. However, the T_g of the PS-rich phase was significantly lower than that of pure PS (373 K),[27] which clearly indicates that, contrary to what is found in PEO/PS blends, there is not complete segregation of the two blocks; this is in agreement with the results reported by O'Malley et al.[28] The use of Fox's equation leads to a weight fraction of PEO in the PS-rich phase on the order of 0.1.

There is another transition in the DSC thermogram near 300 K whose intensity is similar to that of the glass transition of the PEO blocks. O'Malley et al.[28] have reported that in PS-*b*-PEO copolymers with high PS content two melting peaks are found due to the existence of two nucleation mechanisms, however this does no corresponds to the present case. In the second scan, no melting transition is found, even after 1 month aging of the sample; however, the intermediate transition is present. Moreover, its intensity increases when the sample is aged at 313 K. A possible explanation of this

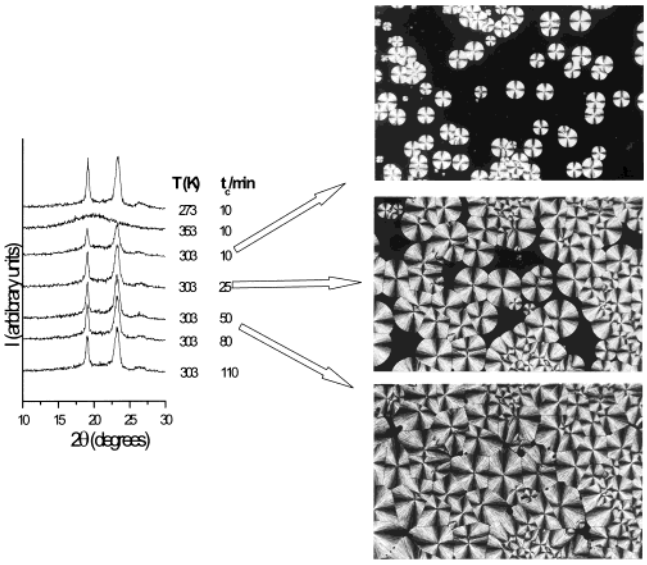

Figure 2. WAXS and polarized optical microscopy results for the crystallization process of the P2 sample at 303 K. The two first diffractograms (from above) correspond to the melting process. T is the temperature at which the diffractogram has been measured, and t_c is the crystallization time.

result is to consider that this transition corresponds to the glass transition of PEO chains tethered to the glassy PS phase. The incomplete segregation of the two blocks would lead to a plastification effect by the PEO blocks which, after a fast vitrification of the PS blocks, would increase slightly with time. However, as it will be discussed below, the dielectric results do not show any evidence for this.

The thermograms of the P2 samples show a very weak glass transition of the PEO chains at low temperatures and a melting peak that is not modified when the sample is cooled from the melt and then remelted. The melting temperature agrees with that obtained in the first scan for the P1 sample and with the values reported in the literature.[7] However, the T_g of PEO is 15 deg higher, thus indicating miscibility (assuming Fox's equation, the weight fraction of PS in the PEO-rich phase might be as high as 0.2). The apparent insensibility of T_m to the mixing of the two blocks may be explained by the results of Yu et al.[12] which point out that there is only amorphous PEO chains in the interface between the crystalline and the amorphous regions.

As already mentioned, the SAXS data obtained show a rather high noise/signal ratio. No structure was found in the intensity vs wavevector curve for the P1 sample in the $T_g(PS) \leq T \leq 400$ K. The two peaks (one of them of very low intensity) obtained for the P2 sample might be compatible with a lamellar structure.[1] The crystallization kinetics of sample P2 has been followed by DSC, WAXS, and polarized optical microscopy. As an example, Figure 2 shows the results obtained for $T_c = 303$ K. As can be observed, in spite of the fact that the degree of crystallinity is 60% (59% from DSC and 62% from WAXS), the spherulites fill the whole sample, which means that the amorphous phase is sandwiched between the lamellae, a fact already discussed by Floudas and Tsilianis[10] and Nogales et al.[18] The data have been fitted to the Avrami equation

$$1 - X = \exp[zt^n] \qquad (1)$$

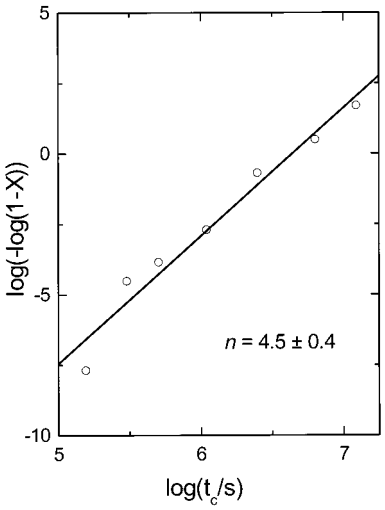

Figure 3. Avrami's plot of the crystallization kinetics of the P2 sample at 303 K. See eq 1. X is the crystalline fraction in the sample, and t_c is the crystallization time.

where the crystallinity fraction X can be calculated from the DSC thermograms ($X = \Delta H(t)/\Delta H^\infty$, where ΔH is the enthalpy of melting at time t and $\Delta H^\infty = 82.95$ J·g^{-1} corresponds to the maximum crystallization for the sample), or from the WAXS diffractograms ($X = S(t)/S_0$, where $S(t)$ is the area under the crystalline peaks and S_0 is the total area under the diffractogram). Figure 3 shows that the results obtained from DSC on heating follow quite closely eq 1 with $n = 4.5 \pm 0.4$, which again is in agreement with the results for the PEO homopolymer.[10]

Figure 4a shows the imaginary part of the permittivity as a function of T and ω (the angular frequency) for the P1 sample. At high temperatures (but below the T_g of the PS blocks), a strong conductivity contribution is found at low frequencies, together with a low intensity process which has been attributed to the structural or α-relaxation of the amorphous PEO chains. As T is decreased the α-process moves toward lower frequencies, and a more intense subvitreous β-relaxation appears. Smith et al.[22] have reported two structural relaxations for composites of PS/PS-*b*-PEO/PEO, however they analyzed the data by making a convolution of the experimental data to different Gaussian peaks, for a broad relaxation peak such as that of the α-process shown in Figure 4a the procedure used by Smith et al.[22] tends to give more than one contribution, and it makes it difficult to conclude whether it actually corresponds to a single broad process or to two sharper ones.

Figure 4b shows the DRS results for the P2 sample. We do not report data above T_m in order to avoid geometrical changes in the capacitor due to the melting of the sample. In any case, for $T > T_m$ only a strong conductivity contribution is seen within the experimental frequency range. For temperatures close to T_m, a slow relaxation MW process appears; this is an important difference from the behavior of the P1 sample. In this temperature range, the slope of the intense conductivity contribution changes significantly. At lower temperatures the structural α- and the subvitreous β-relaxations are found. It must be noticed that the intensity of the MW-relaxation is almost 2 orders of magnitude higher than that of the structural relaxation. Conductivity and polarization contributions have been reported for semicrystalline PEO-*b*-PPO-*b*-PEO copoly-

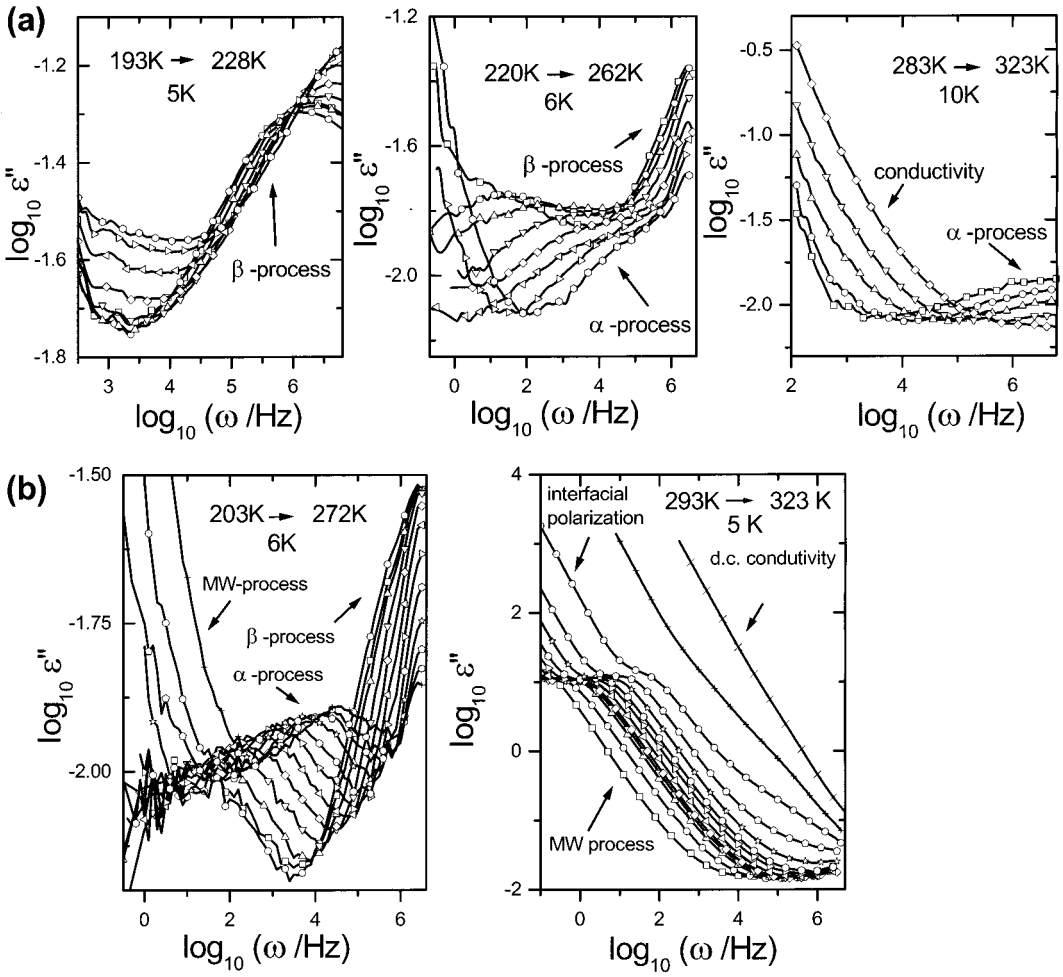

Figure 4. (a) Imaginary part of the dielectric permittivity for copolymer P1. The temperature interval and the step between the isotherms are indicated in the plots. (b) Same plot for copolymer P2. ω is the angular frequency.

mers,[19] but not for PS/PEO and PS/PS-*b*-PEO/PEO composites.[22]

Discussion

To analyze the DRS results, the $\epsilon^*(\omega,T)$ surface has been assumed to be the sum of different contributions. We have assumed that the α-relaxation is described by a Havriliak−Negami function[29]

$$\epsilon^*(\omega) = \epsilon_u + \frac{\Delta\epsilon}{[(1 + i\omega\tau_{HN})^{\delta}]^{\gamma}} \qquad (2)$$

where $\Delta\epsilon = \epsilon_r - \epsilon_u$ is the strength of the relaxation and ϵ_r and ϵ_u are the relaxed and unrelaxed values of ϵ', respectively. δ and γ are dimensionless parameters that describe the symmetric and asymmetric broadening of the loss function $\epsilon''(\omega)$, respectively. They are constrained such as $0 < \delta$, $\delta\gamma \leq 1$. We have found that for the α-, the β-, and the MW-relaxations $\gamma = 1$; i.e., the relaxations can be described by a Cole−Cole function,[29] this is in agreement with previous results for PEO-containing systems above T_m,[30] and in PEO solutions.[31] The conductivity and electrode polarization contributions have been modeled as distributed elements in parallel with the previous contributions. These elements have somewhat different characteristics depending upon the existence and extent of crystalline phase in the sample.[19] The parameters of the different contributions were fitted as in a previous work.[19] In general, it has been possible to fit simultaneously the $\epsilon'(\omega)$ and $\epsilon''(\omega)$ within the experimental uncertainty.

Figure 5 shows the temperature dependence of $\Delta\epsilon_\alpha$ and of the width at half-height w_α for the α-relaxation of both samples, where w_α was calculated from the δ parameter. The intensity of the relaxation decreases with increasing T for the noncrystalline sample and tends to merge with the results for the crystalline sample at temperatures above T_m; this behavior is similar to the one reported in the literature for other polymers. Figure 6 shows the dependence of $\Delta\epsilon_\alpha$ with the percentage of amorphous PEO phase at 220 K; as can be observed, $\Delta\epsilon_\alpha$ would be zero for a fully crystalline sample. Polymers with a noticeable rigid amorphous phase lead to $\Delta\epsilon_\alpha = 0$ for crystallinity degrees lower than 100%.[18] Figure 5 also shows that the α-process is broader in the P1 sample. In principle, this might seem surprising since one might expect the P2 sample to have an important dynamic heterogeneity induced by the crystalline phase (recall that the amorphous phase is sandwiched between the lamellae). However, the DSC results (see Figure 1) show two well-differentiated values of T_g which means that the P1 sample is in fact heterogeneous with a PEO-rich amorphous phase dispersed in a PS-rich glassy phase, and therefore, dynamic heterogeneity is also to be expected. Moreover, as already mentioned, immiscibility is not complete in the amorphous phases, thus leading to further increase of w_{HN} due to concentration fluctuations. For both samples,

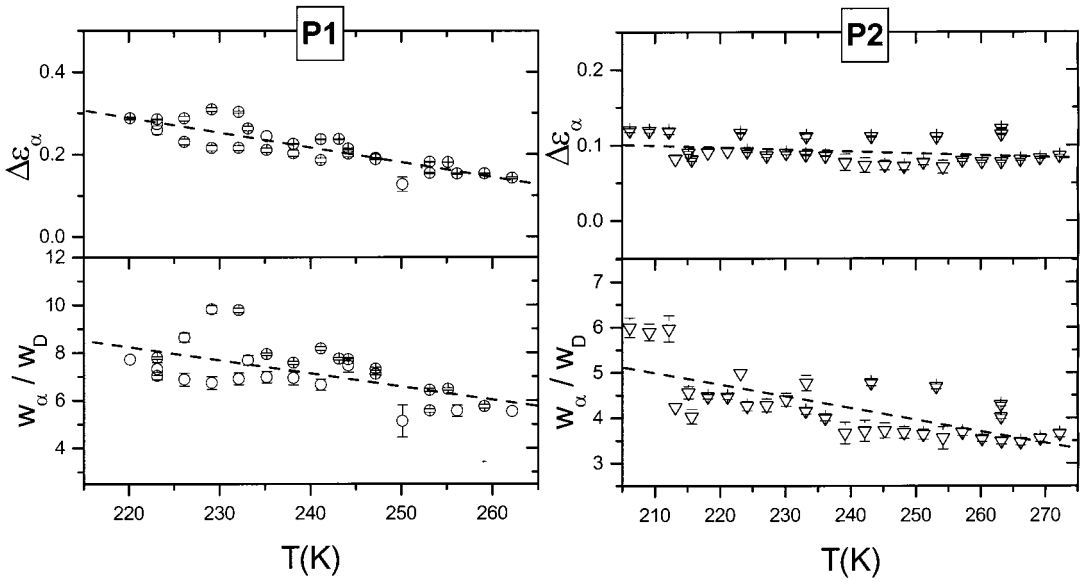

Figure 5. Temperature dependence of the intensity $\Delta\epsilon_\alpha$ and width at half-height w_α for the α-relaxation of copolymers P1 (left) and P2 (right). w_D represents the width of a Debye process (1.14 decades).

w_{HN} increases with decreasing T, which is agreement with the behavior found in most homopolymers.[32]

Figure 7 shows that $\Delta\epsilon_\beta$ and w_β for the β relaxation are rather similar for the two samples; $\Delta\epsilon_\beta$ increases with T while w_{HN} decreases in the temperature range studied, a fact that is not surprising when compared with the behavior usually found in homopolymers.[33] The width of the β transition approaches the value of a Debye process at the highest temperatures.

Figure 8 shows that for the MW process, the intensity increases very slightly with increasing T, while w_{MW} remains essentially constant, and at low temperatures is smaller than the value corresponding to the β process.

Figure 9 shows the relaxation map for the two samples. The relaxation time associated with the maximum of each mode distribution can be calculated from eq 1 as[34]

$$\tau_{max} = \tau_{HN}\left\{\frac{\sin\left[\frac{\pi\delta\gamma}{2(\gamma+1)}\right]}{\sin\left[\frac{\pi\delta}{2(\gamma+1)}\right]}\right\}^{1/\delta} \qquad (3)$$

As can be observed, for the α-relaxation the temperature dependence of τ_{max} is stronger for the P1 copolymer. For the sake of comparison results for different PEO homopolymers and for PEO/PS composites are also included, it can be observed that τ_{max} is quite sensitive to the structure of the sample for the α-relaxation. The temperature dependence of τ_{max} for the P1 sample is similar to those of the PEO samples and of a PS(5%)/PEO(95%) composite. For the PEO samples, the α-relaxation slows down as the molecular weight is decreased as a consequence of the increase of the degree of crystallinity.[35,36] The molecular weight of the PEO chains used in the composite is also 3400, while that of the PS is 104 000; thus, its T_g is above 370 K. It seems that introducing geometrical constraints (either by increasing the crystallinity or introducing a glassy phase in excess) tends to slow the α-transition but does not affect qualitatively the shape of the τ_{max} vs $1/T$ curve. However, the behavior of the P2 sample is different from that described above and is very similar to the one found

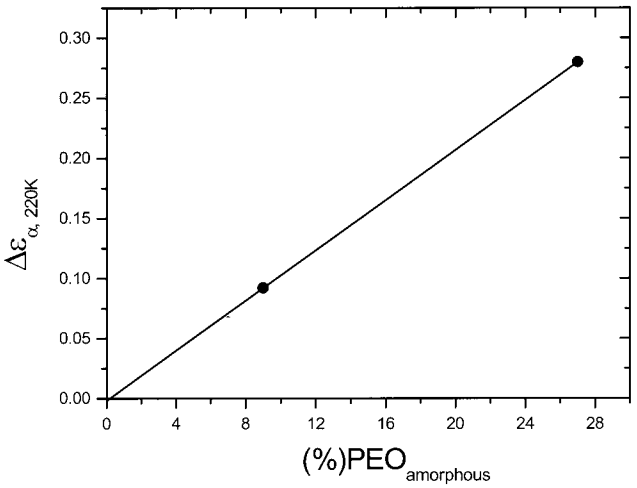

Figure 6. Dependence of the intensity of the α-relaxation, $\Delta\epsilon_\alpha$, with the percentage of amorphous PEO chains in the sample. Notice that for a copolymer with 100% crystalline PEO fraction $\Delta\epsilon_\alpha = 0$.

for the rigid amorphous phase described by Smith et al.[22] in the PS/PEO composite. As it has been discussed above, in the P2 sample the amorphous PEO chains are completely sandwiched by the crystalline lamellae. Thus, it might be appealing to assign the MW relaxation to the rigid amorphous phase of the composite. However, the high intensity of this mode compared to the α mode, its Cole−Cole shape, and the Arrhenius-like behavior of its characteristic relaxation time lead us to associate this relaxation with the Maxwell−Wagner interfacial polarization contribution due to the presence of the crystal interfaces.

In all the cases, the τ_{max} vs $1/T$ curve can be described by the Vogel−Fulcher−Tamman equation

$$\tau_{max} = \tau_0 \exp\left[\frac{DT_0}{T - T_0}\right] \qquad (4)$$

where the preexponential factor τ_0 is on the order of a vibrational frequency, T_0 is the Vogel temperature, and D is the strength parameter, which is related to the

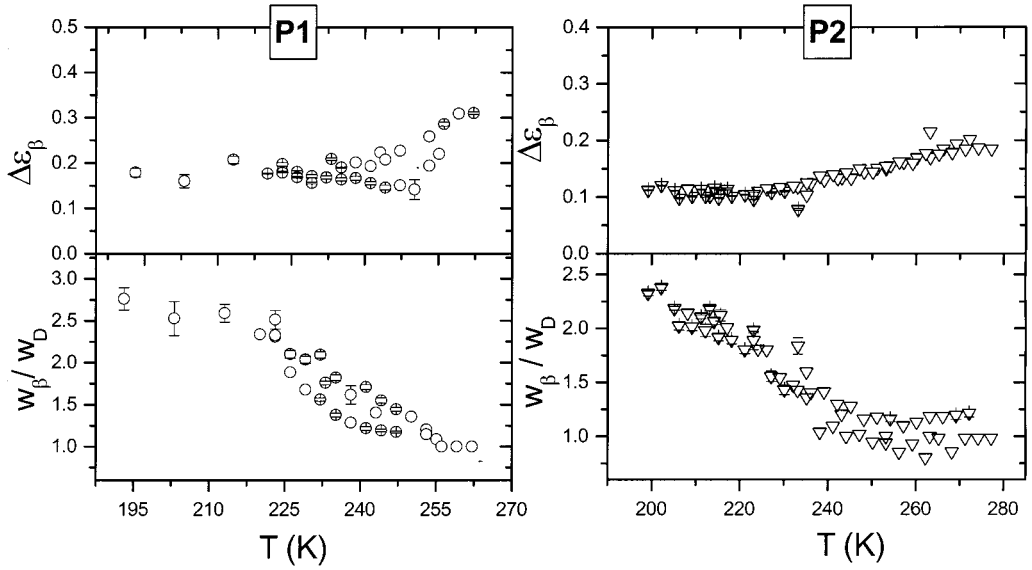

Figure 7. Intensity $\Delta\epsilon_\beta$ and width w_β of the β-relaxation for the copolymer P1 (left) and P2 (right). w_D represents the width of a Debye process.

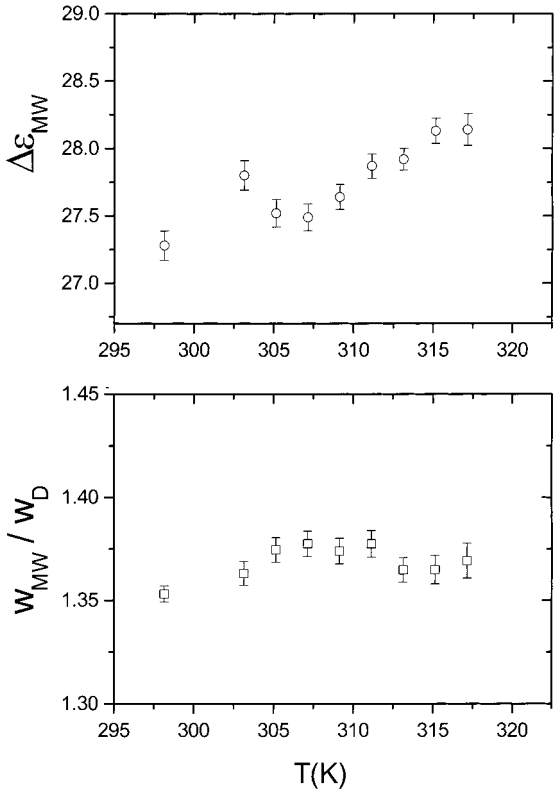

Figure 8. Intensity $\Delta\epsilon_{MW}$ and width w_{MW} of the MW-relaxation for the copolymer P2. w_D represents the width of a Debye process.

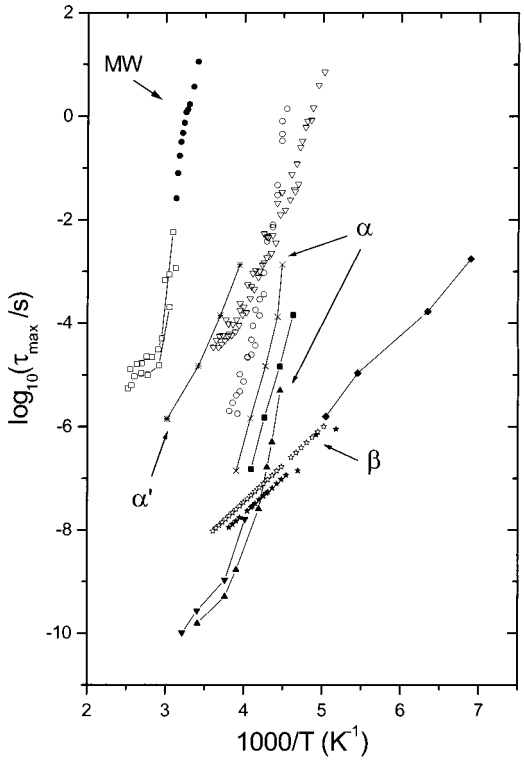

Figure 9. Relaxation map for the two block copolymers studied in this work. τ_{max} is the relaxation time of the maximum of the $\epsilon''(\omega)$ vs ω curves, and T is the temperature. For comparison, data for related systems are included. Symbols: ▽, α-relaxation of sample P2; ○, α-relaxation of sample P1; ▲, α-relaxation of PEO ($M_w = 2.8 \times 10^6$); ▼, α-relaxation of PEO ($M_w = 2.8 \times 10^5$); ■, α-relaxation of PEO ($M_w = 3400$); ×, α-relaxation of PEO in a PS(5%)/PEO(95%) composite; ∗, α_c'-relaxation (rigid amorphous fraction) of PEO in a PS(5%)/PEO(95%) composite; □, α_c-relaxation for PS−PEO diblock copolymers (for the last two symbols we maintain the nomenclature of ref 22 from which the data were taken); ●, MW-relaxation for sample P2; ☆, β-relaxation for sample P1; ★, β-relaxation for sample P2; ◆, β-relaxation for PEO homopolymer.

fragility index m at T_g via $m = [d(\log_{10}\tau_{max})/d(T/T_g)]_{T_g} = [T_g/\log 10]DT_0/(T_g - T_0)^2$. Table 2 shows that the noncrystalline sample has a much larger fragility than the crystalline one (in fact m is unusually low for P2). This result was unexpected for two reasons: (a) it is contrary to what was previously found for PEO-*b*-PPO-*b*-PEO copolymers, where no glassy phase was present at the temperatures studied;[19] (b) the degree of mixing of the PEO-rich regions is larger in P2 than in P1 (at least considering the values of T_g), and the fragility of pure PS is large ($m = 127-139$).[37]

Green et al.[38] have pointed out that m is not the best criterion for measuring the fragility of a glass former; instead they have proposed to use $F_{1/2} = 2[T_g/T_{1/2} - 0.5]$,

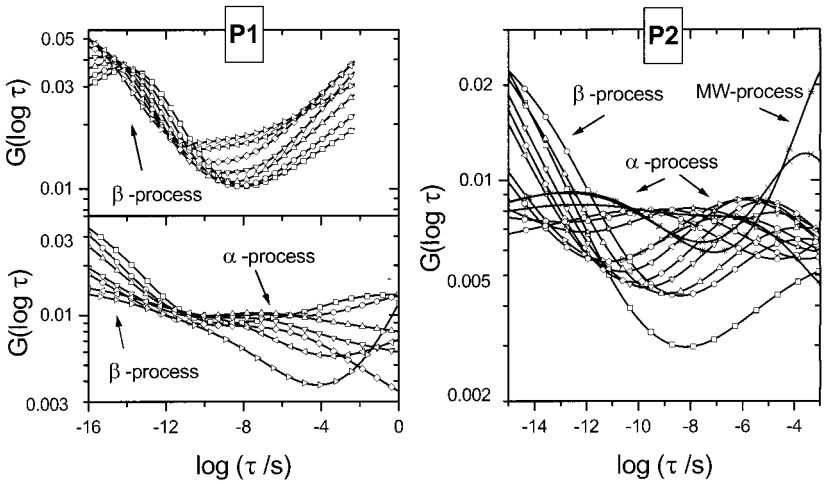

Figure 10. Unnormalized retardation spectra $G(\log \tau)$ for the two PEO-*b*-PS-*b*-PEO copolymers studied in this work. τ is the retardation time. The temperature ranges are the same as those in Figure 4, except for the fact that the interval for which the conductivity contributions are noticeable has not been included.

Table 2. Parameters That Best Describe the Temperature Dependence of the Relaxation Times of the α- and *β*-Relaxations of the Two Copolymers

copolymer	$\log(\tau_0/\mathrm{s})$	D	T_0/K	m	$F_{1/2}$
P1	-9 ± 1	2.6 ± 0.9	197 ± 6	119	0.60
P2	-9.0 ± 0.5	9 ± 2	143 ± 8	43	0.2

where it is considered that $\tau_{max}(T_g) = 10^2$ s, and $\tau_{max}(T_{1/2}) = 10^{-6}$ s. Moreover, Ito et al.[39] have suggested that there is a correlation between $F_{1/2}$ and $\Delta T_g/T_g$, as obtained from DSC. Table 2 gives the values of $F_{1/2}$ for the two samples; while the value for the P1 sample is quite similar to that of the PEO-*b*-PPO-*b*-PEO copolymers (0.69 ± 0.02), the value for the P2 sample is quite small and does not fulfill Ito's correlation, a fact already found by Ngai and Yamamuro for other systems.[40] Finally, it must be said that the temperature dependence of τ_{max} of the two copolymers is compatible with the description recently proposed by Colby.[41]

The behavior of the β- and MW-relaxations (α_c-relaxations according to ref 22) is similar in all the samples, and the temperature dependence is of Arrhenius type. A consequence of the previous analysis is that the α- and β-relaxations would merge at a lower temperature for the P1 sample than for the P2 one.

As an alternative to the phenomenological description of $\epsilon^*(\omega)$ described above, it is possible to carry out the analysis of the data in terms of the (unnormalized) retardation spectrum $G(\log \tau)$:

$$\epsilon^* - \epsilon_u = \int \frac{G(\log \tau)}{1 + i\omega\tau} \mathrm{d}(\log \tau) \qquad (5)$$

We have calculated $G(\log \tau)$ using the regularization algorithm proposed by Weese.[42] Figure 10 shows the spectra obtained for the two samples over the temperature interval studied, the method is able to identify the different contributions when no large conductivity contributions are present (otherwise very large uncertainties are obtained). The results obtained for $\Delta\epsilon$, w_{HN}, and the τ_{max} of the α, β, and MW processes are in good agreement with those obtained from the phenomenological analysis.

Conclusions

DSC and WAXS data show that PEO-*b*-PS-*b*-PEO copolymers with PS blocks larger than the PEO ones may be crystalline when precipitated from solution but do not crystallize from melt. Two well-differentiated glass transitions confirm that the copolymers are heterogeneous, but there is a slightly larger miscibility than in PS/PEO blends. When the molecular weights of the blocks are similar, the copolymer crystallizes either from solution or from the melt. The exponent of the Avrami's equation indicates that the crystallization takes place by a homogeneous nucleation with 3-D nuclei. The lamellae fill the whole sample (for 60% degree of crystallinity) thus the amorphous phase is sandwiched between the lamellae.

The existence of the PEO-crystalline or the glassy PS-rich phases do not seem to affect the dynamics of the subvitreous β-relaxation. Also the dynamics of the PEO chains included in the lamellae seem to be insensitive to whether the sample is a block copolymer or a blend. The structural transition of the amorphous PEO chains is sensitive to the structure of the sample, and very different fragilities are found for the crystalline and the amorphous copolymers. However, the comparison with the results obtained for PEO-*b*-PPO-*b*-PEO copolymers indicates that the relation between the structure and the fragility, if any, is not straightforward.

Acknowledgment. This work was supported in part by DGICYT under Grant BQU2000-786, and by Fundación Areces. We are grateful to Dr. M. G. Prolongo for the use of the DSC, to Dr. F. Conde for his help with the WAXS measurements, and to J. A. R. Cheda for the help with the optical microscopy. S.M. was supported by a FPI fellowship.

References and Notes

(1) Hamley, I. W. *The Physics of Block Copolymers*; Oxford University Press: Oxford, England, 1998.
(2) Cristal, R. G.; Erhardt, P. F.; O'Malley, J. J. In *Block Copolymers*; Aggarwal, S. L., Ed.; Plenum: New York, 1970; p 179.
(3) *Block copolymers*; Baltá Calleja, F. J., Roslaniec, Z., Eds.; Marcel Dekker: New York, 2000.
(4) Cohen, R. E.; Cheng, P. L.; Douzinas, K.; Kofinas, P.; Berney, C. V. *Macromolecules* **1990**, *23*, 324.
(5) Sakurai, K.; MacKnight, W. J.; Lohse, K. J.; Schulz, D. N.; Sissano, J. A.; Lin, J. S.; Agamalyan, M. *Polymer* **1996**, *37*, 4443.
(6) Quiram, D. J.; Register, R. A.; Marchand, G. R.; Adamson, D. H. *Macromolecules* **1998**, *31*, 4891.

(7) Hong, S.; Yang, L.; MacKnight, W. J.; Gido, S. P. *Macromolecules* **2001**, *34*, 7009.
(8) Zhu, L.; Chen, A.; Zhang, A.; Calhoun, B. H.; Chun, M.; Chang, S. Z. D.; Quirk, B. S.; Yeh, F.; Hashimoto, T. *Phys. Rev. B* **1999**, *60*, 10022.
(9) Zhu, L.; Cheng, S. Z. D.; Calhoun, B. H.; Ge, Q.; Quirk, R. P.; Thomas, E. L.; Hsiao, B. S.; Yeh, F.; Lotz, B. *J. Am. Chem. Soc.* **2000**, *122*, 5957.
(10) Floudas, G.; Tsitsilianis, C. *Macromolecules* **1997**, *30*, 4381.
(11) Kyritsis, A.; Pisis, P.; Mai, S.-M.; Booth, C. *Macromolecules* **2000**, *33*, 4581.
(12) Yu, H.; Natansohn, A.; Singh, M. A.; Torriani, I. *Macromolecules* **2001**, *34*, 1258.
(13) Karatasos, K.; Anastasiadis, S. H.; Floudas, G.; Fytas, G.; Pispas, H.; Hadjichristidis, H.; Pakula, T. *Macromolecules* **1996**, *29*, 1326.
(14) Dobbertin, J.; Hannermann, J.; Schick, C.; Pötter, M.; Dehne, H. *J. Chem. Phys.* **2000**, *108*, 9062.
(15) Kotaka, T.; Adachi, K. *Macromol. Symp.* **1997**, *124*, 3.
(16) Alig, I.; Kremer, F.; Fytas, G.; Roovers, J. *Macromolecules* **1992**, *25*, 5277.
(17) Vogt, S.; Gerharz, G.; Fischer, E. W.; Fytas, G. *Macromolecules* **1992**, *25*, 5986.
(18) Nogales, A.; Ezquerra, T. A.; García, J. M.; Baltá-Calleja, F. J. *J. Polym. Sci., Part B: Polymer Phys.* **1999**, *37*, 37.
(19) Moreno, S.; Rubio, R. G.; Luengo, G.; Ortega, F.; Prolongo, M. G. *Eur. Phys. E* **2001**, *4*, 173.
(20) Chow, T. S. *Macromolecules* **1990**, *23*, 333.
(21) Martuscelli, F.; Silvestre, C.; Addonizio, M. L.; Amelino, I. *Makromol. Chem.* **1986**, *187*, 1557.
(22) Smith, T. W.; Abkowitz, M. A.; Conway, G. C.; Luca, D. J.; Serpico, J. M.; Wnek, G. E. *Macromolecules* **1996**, *29*, 5042; **1996**, *29*, 5046.
(23) Mijovic, J.; Sy, J.-W.; Kwei, T. K. *Macromolecules* **1997**, *30*, 3042.
(24) Hatakeyama, T.; Quinn, F. X. *Thermal Analysis*, 2nd ed.; Wiley: New York, 1999.
(25) *Handbook of Polymers*, 4th ed.; Brandrup, J., Immergut, E. H., Grulke, E. A., Eds.; John Wiley & Sons: New York, 1999.
(26) Suzuki, H.; Wunderlich, B. *J. Polym. Sci.: Polym. Phys. Ed.* **1985**, *23*, 1671.
(27) McCrum, N. G.; Read, B. E.; Williams, G. *Anelastic and Dielectric Effects in Polymeric Solids*; Dover: New York, 1991.
(28) O'Malley, J. J.; Crystal, R. G.; Erhart, P. F. In *Block Copolymers*; Aggarwal, S. L.; Ed.; Plenum: New York, 1970; p 163.
(29) Havriliak, S.; Havriliak, S. J. *Dielectric and Mechanical Relaxations in Materials. Analysis and Application to Polymers, their Solutions and Other Systems*; Hanser Verlag: New York, 1996.
(30) Sengwa, R. J.; Kaur, K.; Chaudhary, R. *Polym. Int.* **2000**, *49*, 599.
(31) Shinyashiki, N.; Sudo, S.; Abe, W.; Yagihara, S. *J. Chem. Phys.* **1998**, *109*, 9843.
(32) Chamberlain, R. V. *Phase Transitions* **1998**, *65*, 169.
(33) Schönhals, A. In *Dielectric Spectroscopy of Polymeric Materials. Fundamentals and Applications*; Runt, J. P., Fitzgerald, J. J., Eds.; American Chemical Society: Washington, DC, 1977.
(34) Díaz Calleja, R. *Macromolecules* **2000**, *33*, 8924.
(35) Boyd, R. H. *Polymer* **1985**, *26*, 323.
(36) Ngai, K. L. *J. Chem. Phys.* **1998**, *109*, 6982.
(37) Hempel, E.; Hempel, G.; Hensel, A.; Schick, C.; Donth, E. *J. Phys. Chem. B* **2000**, *104*, 2460.
(38) Green, J. L.; Ito, K.; Xu, K.; Angel, C. A. *J. Phys. Chem. B* **1999**, *103*, 3991.
(39) Ito, K.; Moynihan, C. T.; Angel, C. A. *Nature* **1999**, *398*, 492.
(40) Ngai, K. L.; Yamamuro, O. *J. Chem. Phys.* **1999**, *111*, 10403.
(41) Colby, R. H. *Phys. Rev. E* **2000**, *61*, 1783.
(42) Weese, J. *Comput. Phys. Commun.* **1993**, *77*, 429.

MA011732U